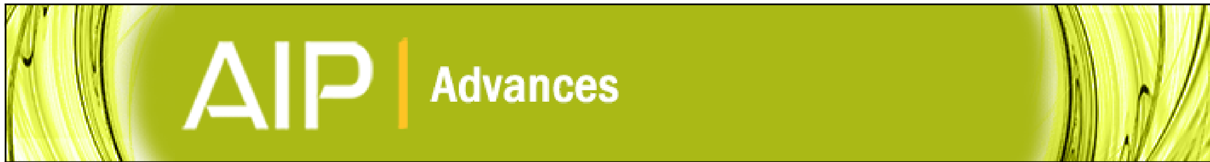

Nanospherical-lens lithographical Ag nanodisk arrays embedded in p-GaN for localized surface plasmon-enhanced blue light emitting diodes

Tongbo Wei, Kui Wu, Ding Lan, Bo Sun, Yonghui Zhang, Yu Chen, Ziqiang Huo, Qiang Hu, Junxi Wang, Yiping Zeng, and Jinmin Li

Citation: AIP Advances **4**, 067119 (2014); doi: 10.1063/1.4882179
View online: http://dx.doi.org/10.1063/1.4882179
View Table of Contents: http://scitation.aip.org/content/aip/journal/adva/4/6?ver=pdfcov
Published by the AIP Publishing

Articles you may be interested in

Fabrication and optical characteristics of phosphor-free InGaN nanopyramid white light emitting diodes by nanospherical-lens photolithography
J. Appl. Phys. **115**, 123101 (2014); 10.1063/1.4869336

Selectively grown photonic crystal structures for high efficiency InGaN emitting diodes using nanospherical-lens lithography
Appl. Phys. Lett. **101**, 211111 (2012); 10.1063/1.4767334

Localized surface plasmon-enhanced ultraviolet electroluminescence from n-ZnO/i-ZnO/p-GaN heterojunction light-emitting diodes via optimizing the thickness of MgO spacer layer
Appl. Phys. Lett. **101**, 142101 (2012); 10.1063/1.4757127

Localized surface plasmon-enhanced electroluminescence from ZnO-based heterojunction light-emitting diodes
Appl. Phys. Lett. **99**, 181116 (2011); 10.1063/1.3658392

Surface plasmon-enhanced light-emitting diodes with silver nanoparticles and SiO2 nano-disks embedded in p-GaN
Appl. Phys. Lett. **99**, 041107 (2011); 10.1063/1.3616149

All article content, except where otherwise noted, is licensed under a Creative Commons Attribution 3.0 Unported license. See: http://creativecommons.org/licenses/by/3.0/
Downloaded to IP: 159.226.231.80 On: Tue, 02 Sep 2014 07:34:08

AIP ADVANCES **4**, 067119 (2014)

Nanospherical-lens lithographical Ag nanodisk arrays embedded in *p*-GaN for localized surface plasmon-enhanced blue light emitting diodes

Tongbo Wei,[1,a] Kui Wu,[1] Ding Lan,[2] Bo Sun,[1] Yonghui Zhang,[1] Yu Chen,[1] Ziqiang Huo,[1] Qiang Hu,[1] Junxi Wang,[1] Yiping Zeng,[1] and Jinmin Li[1]
[1]*State Key Laboratory of Solid-State Lighting, Institute of Semiconductors, Chinese Academy of Sciences, Beijing, 100083, China*
[2]*National Microgravity Laboratory, Institute of Mechanics, Chinese Academy of Sciences, Beijing, 100080, China*

(Received 18 March 2014; accepted 28 May 2014; published online 5 June 2014)

Large-scale Ag nanodisks (NDs) arrays fabricated using nanospherical-lens lithography (NLL) are embedded in *p*-GaN layer of an InGaN/GaN light-emitting diode (LED) for generating localized surface plasmon (LSP) coupling with the radiating dipoles in the quantum-well (QWs). Based on the Ag NDs with the controlled surface coverage, LSP leads to the improved crystalline quality of regrowth *p*-GaN, increased photoluminescence (PL) intensity, reduced PL decay time, and enhanced output power of LED. Compared with the LED without Ag NDs, the optical output power at a current of 350 mA of the LSP-enhanced LEDs with Ag NDs having a distance of 20 and 35 nm to QWs is increased by 26.7% and 31.1%, respectively. The electrical characteristics and optical properties of LEDs with embedded Ag NPs are dependent on the distance of between Ag NPs and QWs region. The LED with Ag NDs array structure is also found to exhibit reduced emission divergence, compared to that without Ag NDs. © *2014 Author(s). All article content, except where otherwise noted, is licensed under a Creative Commons Attribution 3.0 Unported License.* [http://dx.doi.org/10.1063/1.4882179]

I. INTRODUCTION

Nitride wide bandgap light-emitting diodes (LEDs) have recently attracted considerable interest due to their various applications, such as traffic signals, back-side lighting and illumination lighting by white light LEDs. Though great success has been achieved in improving LEDs performance, there are still critical issues to increase the efficiency and reduce the price and power consumption of LEDs for more advanced applications. This makes it desirable to increase the internal quantum efficiency (η_{int}) and light extraction efficiency ($\eta_{extraction}$). Among many recent approaches to the improvement of η_{int}, the coupling between localized surface plasmons (LSPs) and InGaN/GaN multiple-quantum-wells (MQWs) is a promising way to increase the spontaneous emission rate.[1–5] LSPs are local collective oscillations of the electrons at interfaces between metal nanoparticles (NPs) and a dielectric matrix. The resonant excitation of LSPs leads to selective photon absorption and enhancement of local electromagnetic fields near metal nanoparticles. For the LSPs enhancement to be efficient, the NPs layer should be placed in close proximity to the active MQWs region, generally no further than 40–50 nm.[6] Recently, many LSPs-LEDs have been demonstrated by embedding Au or Ag NPs in either *n*-GaN or *p*-GaN layer for shortening the distance between the MQWs and the metal NPs.[7–10] However, these metal NPs are usually fabricated by the thermal annealing process of thin metal layer such as Au, Ag or Pt, without controlling the size and shape. At the circumstance,

[a]Author to whom correspondence should be addressed. Electronic mail: tbwei@semi.ac.cn, Tel.: +86-10-82305304, Fax: +86-10-82305245.

 © Author(s) 2014

All article content, except where otherwise noted, is licensed under a Creative Commons Attribution 3.0 Unported license. See: http://creativecommons.org/licenses/by/3.0/
Downloaded to IP: 159.226.231.80 On: Tue, 02 Sep 2014 07:34:08

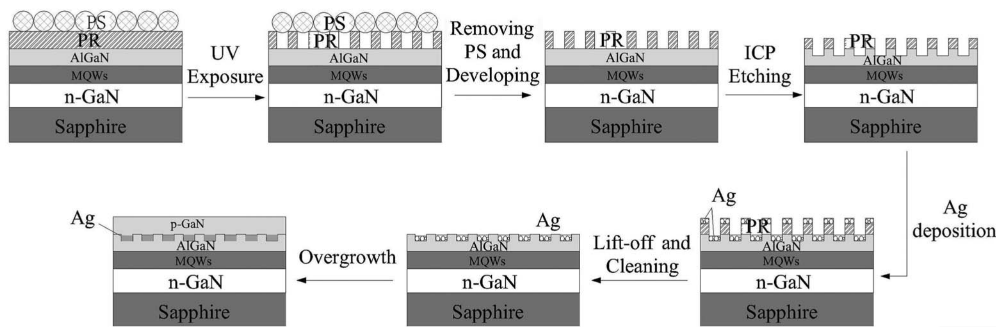

FIG. 1. Schematic flowchart of the LSP-enhanced blue LEDs with Ag NDs embedded in *p*-GaN layer.

the random distribution and high surface coverage of metal NPs on the GaN surface deteriorate the subsequent re-growth quality of MQWs or *p*-GaN and degrade electrical characteristics of LSP-enhanced LEDs. On the other hand, Henson et. al. reported that two-demensional arrays of silver nanocylinders with highly controlled dimensions were used to demonstrate plasmon-enhanced near-green emission and the resonance wavelength may be tuned by the change of nanocylinder size.[11,12] However, it is a pity that the controlled nanocylinders are fabricated by electron-beam lithography, which is expensive and low throughput.

In previous report, nanoscale triangular prisms with a controlled size have been fabricated to generate LSP effect by nanosphere lithography.[13] Here, we introduce an alternative method of nanospherical-lens lithography (NLL)[14,15] instead of thermal annealing, to produce Ag nanodisks (NDs) arrays with the controlled size and surface coverage. The NLL technology is a simple and economic process, using the single layer transparent polystyrene (PS) spheres as optical lenses to generate sub-wavelength holes on photoresist (PR) by focusing UV light. By NLL technology to fabricate a variety of nano-holes for filling in Ag metal, we can control the surface coverage and size of Ag NDs. In this work, the LSP-enhanced blue LEDs are presented with Ag NDs embedded in *p*-GaN by the selective nano-overgrowth of two-dimensional hole arrays. The optical output power of LEDs with Ag NDs is obviously increased via the LSP resonance coupling between the excitons in MQWs and metal NDs. The electrical characteristics and optical properties of LEDs with embedded Ag NDs are dependent on the distance of between Ag NDs and QWs region.

II. EXPERIMENTAL

The blue InGaN/GaN LEDs were grown on a *c*-plane sapphire by metalorganic chemical vapor deposition (MOCVD). After growth of a 30 nm thick GaN nucleation layer at 550 °C, a 2 μm thick undoped GaN layer and a 2 μm thick *n*-GaN layer were grown at 1030 °C. Then, eight periods of $In_{0.2}Ga_{0.8}N$/GaN multiple quantum wells (MQWs) were grown at 740 °C, followed by the growth of a 20 nm thick *p*-GaN layer at 950 °C as a space layer and finally $Al_{0.2}Ga_{0.8}N$ of 40 nm in thickness was grown at 950 °C as electron blocking layer. The LSP-enhanced LEDs with Ag NDs embedded in *p*-GaN by NLL are fabricated according to the process flow illustrated in Fig. 1. First, a self-assembled monolayer of PS nanospheres with a diameter of 700 nm was formed on the sample surface with a closely packed mode, on which the 500-nm-thick photoresist AR-P 3120 had been spun and baked on a hotplate at 90 °C for 15 min. Then, the wafer was UV-exposed for 2–3 s using a conventional photolithography instrument. After the elimination of PS by ultrasonication in deionized water, the wafer was developed in the diluted AR 300-26 developer and the size of air holes on PR may be tuned by controlling the developing time. Next, the patterned PR served as the mask for etching of the AlGaN layer by inductively coupled plasma (ICP) for 9 s, to transfer the hole array on the LED surface. Subsequently, 30 nm thick Ag layer are evaporated on patterned PR by electron-beam evaporation. Lift-off process was then carried out by dissolving the PR in acetone for 30 min, which produced the arrays of Ag NPs. Then a 40-nm-thick *p*-GaN layer was deposited in the MOCVD chamber at 880 °C as a capping layer and a 140-nm-thick *p*-GaN layer was grown

All article content, except where otherwise noted, is licensed under a Creative Commons Attribution 3.0 Unported license. See: http://creativecommons.org/licenses/by/3.0/
Downloaded to IP: 159.226.231.80 On: Tue, 02 Sep 2014 07:34:08

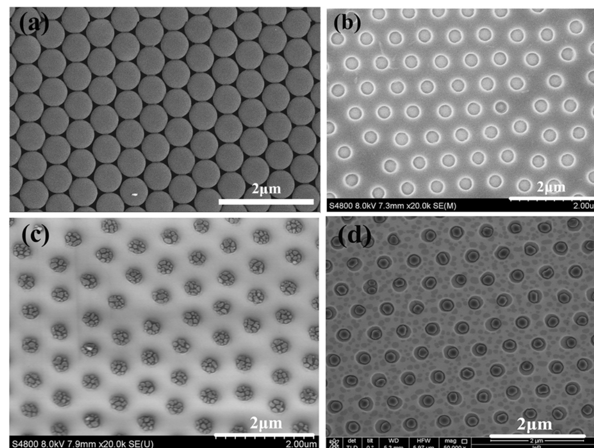

FIG. 2. Plan-view SEM images of (a) uniform close-packed monolayer of PS nanospheres with 700-nm period and (b) PR nanoholes after developing. (c) Ag NPs arrays after Ag deposition on ICP-etched PR and lift-off. (d) Ag NDs arrays formed after the temperature reaches the p-GaN growth temperature.

on the *p*-GaN capping layer at 950 °C. After the selective regrowth of 180 nm thick *p*-GaN layer, the Ag NDs in the hole array were fully covered by the *p*-GaN epilayer. Finally, the LSP-enhanced LED chips were fabricated with a mesa of 1 × 1 mm^2 using our previously reported process[16] and studied with an Everfin-PMS50 spectrum analyzer.

Top-view scanning electron microscopy (SEM) images of monolayer of PS nanospheres with 700-nm period, the hole arrays on PR by NLL and resulting Ag nanostructures are shown in Fig. 2. A large area of highly uniform round-shaped holes of about 320 nm diameter with an undercut can be generated, which completely penetrate through the 500 nm thick PR in Fig. 2(b). The hole diameter could be controlled with varying the exposure and developing time of PR. When the 30-nm-thick Ag thin film is deposited on the ICP-etched PR, Ag nanoparticle arrays can be obtained after lift-off, without using the conventional thermal annealing, as shown in Fig. 2(c). The Ag NPs are well confined in the holes of the *p*-GaN, with a diameter in the range of 50–200 nm. If the 30 nm Ag thin film is directly deposited on the un-ICP PR, round Ag nanodisk can also be obtained after lift-off. However, the weak bonding of Ag nanodisk and GaN surface usually leads to the desquamation with large area during the lift-off process. Therefore, the ICP etching process must be adopted. Furthermore, the configuration of Ag NPs would change during the *p*-GaN growth. As the temperature is increased to the *p*-GaN growth temperature of 880 °C, Ag NPs have melted and formed the Ag nanodisks array as shown in Fig. 2(d). The SEM images demonstrate that selective filling in the recessed hole by ICP etching can economically fabricate high-quality NDs that cover large areas. No Ag particles get out of the holes during the high temperature growth of *p*-GaN and thus don't deteriorate the re-growth of *p*-GaN for LED.

III. RESULTS AND DISCUSSION

After the overgrowth of a 180 nm thick *p*-GaN, the full coalescence of the *p*-GaN layer is achieved for the LSP-enhanced LEDs embedded with Ag NDs. To evaluate the crystalline quality of regrown *p*-GaN, atomic force microscopy (AFM) is used to observe the wet-chemically etched surface of the LEDs embedded without and with Ag NDs in the boiled H_2SO_4 for 1 min. As shown in Fig. 3, it is clearly seen that a lower density of etching pits appears ($\sim1.8 \times 10^9$ cm^{-2}) in the *p*-GaN layer embedded with Ag NDs having a distance of 35 nm to QWs, compared to that of LED without Ag NDs ($\sim3.9 \times 10^9$ cm^{-2}). The observed etching pits with inverted hexagonal pyramid shape are related to the mixed and screw dislocations. The reduction of etching-pit density for *p*-GaN with Ag NDs is ascribed to nanoepitaxial lateral overgrowth (NELO) process in which the surface recessed hole filled with Ag NDs serves as a nanomask similarly to the growth on nanopatterned GaN.[17]

All article content, except where otherwise noted, is licensed under a Creative Commons Attribution 3.0 Unported license. See: http://creativecommons.org/licenses/by/3.0/
Downloaded to IP: 159.226.231.80 On: Tue, 02 Sep 2014 07:34:08

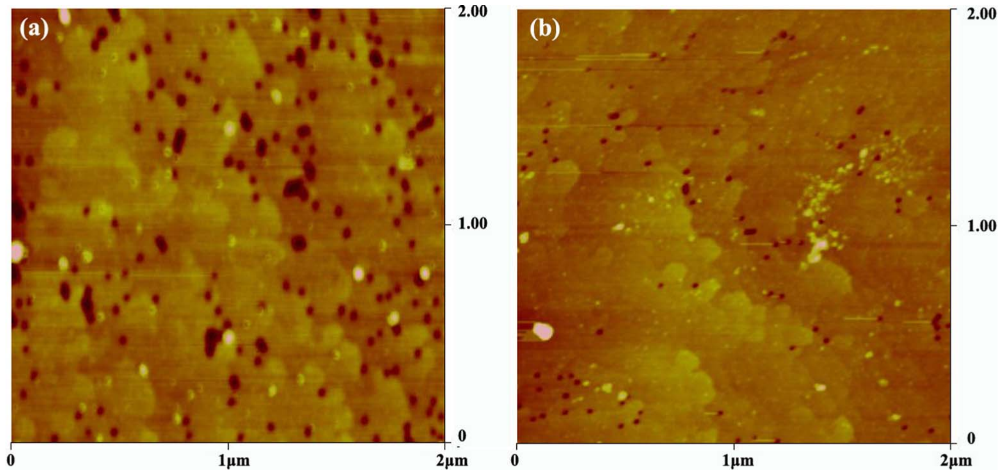

FIG. 3. AFM images of the etched *p*-GaN layer embedded (a) without and (b) with Ag NDs having a distance of 35 nm to QWs in LSP-enhanced LEDs.

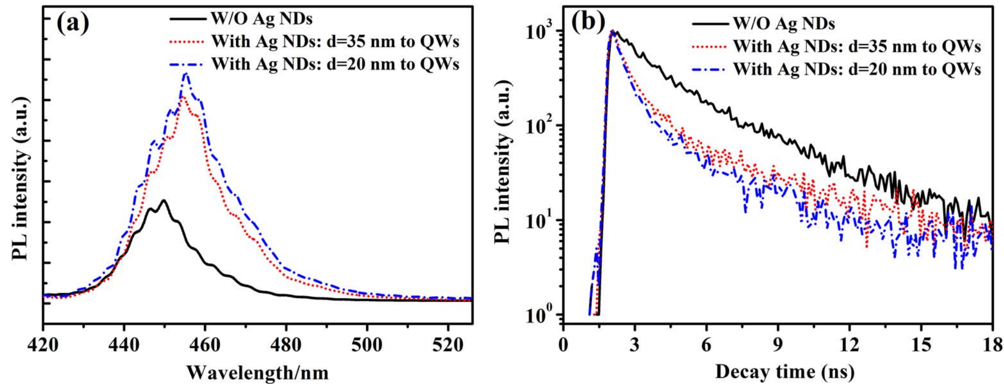

FIG. 4. PL spectra (a) and TRPL spectra (b) of LSP-enhanced LEDs without and with Ag NDs. The distance between the NDs and QWs is 20 nm and 35 nm, respectively.

Here, the selective regrowth may improve the crystalline quality of the subsequent *p*-GaN layer, not the formation of more defects induced by the regrowth over metal NPs in the previous report.[6]

Figure 4 shows the photoluminescence (PL) spectra and time-resolved PL (TRPL) spectra of LSP-enhanced LEDs without and with Ag NDs embedded in *p*-GaN. The PL spectra were measured from the top side of the samples at room temperature using a 405 nm laser. As shown in Fig. 4(a), the PL intensity of the LEDs with Ag NDs is much higher than that of the LED without Ag NDs. For the LEDs with Ag NDs having a distance of 20 nm and 35 nm, the integrated PL intensity is increased by 1.6 and 1.2 times, respectively, compared with that of LED without Ag NDs. The large increase in PL intensity can be attributed to the coupling effects because of the charge density oscillations of the confined SP modes in the Ag NDs.[1] Furthermore, the PL peak of LSP-enhanced LEDs with Ag NPs is red-shifted by about 6 nm in comparison with that of an LED without Ag NDs, which is due to the more enhancement of PL intensity in the longer-wavelength portion of the PL emission by the QW-LSP coupling.[18] To further understand the QW-SP coupling process, Fig. 4(b) compares the TRPL decay curves of LSP-enhanced LEDs without and with Ag NDs embedded in the *p*-GaN. The light source is a Ti:sapphire laser with a nominal wavelength of 375 nm, pulse repetition frequencies of 20 MHz and pulse period of 50 ns. Based the double exponential decay model,[19] the fast part of each decay curve is fitted with a monoexponential decay model to investigate the resonance coupling between excitons in the MQWs and LSPs of the Ag NDs. The decay time of LEDs with Ag NDs having a distance of 20 and 35 nm to QWs is 0.65 ns

All article content, except where otherwise noted, is licensed under a Creative Commons Attribution 3.0 Unported license. See: http://creativecommons.org/licenses/by/3.0/
Downloaded to IP: 159.226.231.80 On: Tue, 02 Sep 2014 07:34:08

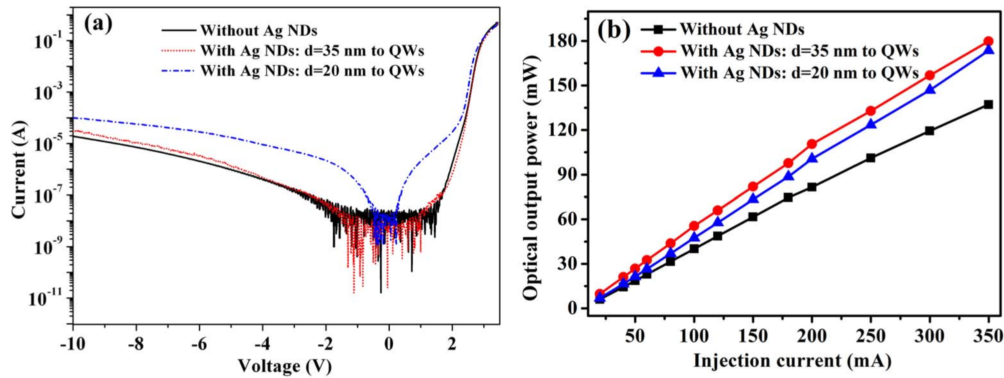

FIG. 5. (a) The reverse and forward *I-V* characteristics of the LSP-enhanced LEDs without and with Ag NDs, having a distance of 20 and 35 nm to QWs on a logarithmic scale. (b) Optical output power of LSP-enhanced LEDs as a function of injection current.

and 0.75 ns, respectively, whereas that of LED without Ag NPs is 1.64 ns. The pronounced decrease in the former lifetime is in full agreement with plasmon-enhanced light emission. Due to the shortening of decay lifetime, fewer carriers are captured at the dislocation location through nonradiative recombination processes and η_{int} is correspondingly increased.

Figure 5(a) shows the logarithmic *I-V* curves of the LSP-enhanced LEDs without and with Ag NDs. At an injection current of 350 mA, the forward bias voltages of LSP-enhanced LEDs without and with Ag NDs having a distance of 20 nm and 35 nm to QWs are almost identical, 3.28 V, 3.33 V and 3.31 V, respectively. However, the forward leakage current for the LED embedded Ag NDs with a 20 nm distance to QWs is larger than others at voltages smaller than 2 V. The shunt bulk leakage paths in GaN-based LEDs usually include dislocation and deep-level traps in the cladding layer. Here, the excess currents in the region ($<$2 V) are dominated by a carrier recombination in depletion regions through trap levels produced by ICP damage at short range of 20 nm from QWs. On the other hand, the LED embedded Ag NDs with a 35 nm distance to QWs shows the almost same forward and reverse leakage current as that of LED without Ag. Therefore, the ICP etching with proper depth and the subsequent regrowth of *p*-GaN over metal NDs do not degrade the electrical properties of LSP-enhanced LEDs. Figure 5(b) shows the optical output power of the three different LEDs as a function of the injection current. Compared with LED without Ag NDs, the optical output power at a current of 350 mA of the LSP-enhanced LEDs with Ag NDs having a distance of 20 nm and 35 nm to QWs is increased by 26.7% and 31.1%, respectively. The enhancement of optical output power can be attributed to an improvement of η_{int} in MQWs owing to an increase in the spontaneous emission rate by the resonance coupling between the excitons and the LSPs in the Ag NDs. It is also noted that the probability of coupling between the excitons in MQWs and LSPs is increased with decreasing the distance from Ag NDs to QWs as shown in PL spectra. However, the electroluminescence (EL) enhancement shows the opposite tendency due to the severe leakage current caused by etching damage in the vicinity of QWs.

As a consequence, the emission efficiency of LED with Ag NDs is increased by direct energy transfer from electron-hole pairs, but part of light is absorbed by Ag NDs. To further understand the influence of Ag NDs on LEDs, we also measured the far-field light output radiation patterns of the LSP-enhanced LED with and without Ag Nds to further investigate the optical effect of Ag NDs on the light output, at a driving current of 200 mA. As determined from the radiation patterns in Fig. 6, the full-width-at-half maximum (FWHM) of emission divergence for LSP-enhanced LED with and without Ag NDs are 146.3° and 151.6°, respectively. It is worth noting that the light is effectively redirected to the top escape cone of the LED through Ag NDs arrays, resulting in the smaller divergent angle. Similar to the photonic crystal (PhC) structures,[20] the Ag NDs arrays embedded in *p*-GaN help to confine the light to radiate in vertical direction. Here, not to directly increase the light extraction efficiency, the Ag NDs arrays may modify the radiation pattern of LEDs. The surface plasmon dispersion engineering depends strongly on the structure, lateral dimension, and height of

All article content, except where otherwise noted, is licensed under a Creative Commons Attribution 3.0 Unported license. See: http://creativecommons.org/licenses/by/3.0/
Downloaded to IP: 159.226.231.80 On: Tue, 02 Sep 2014 07:34:08

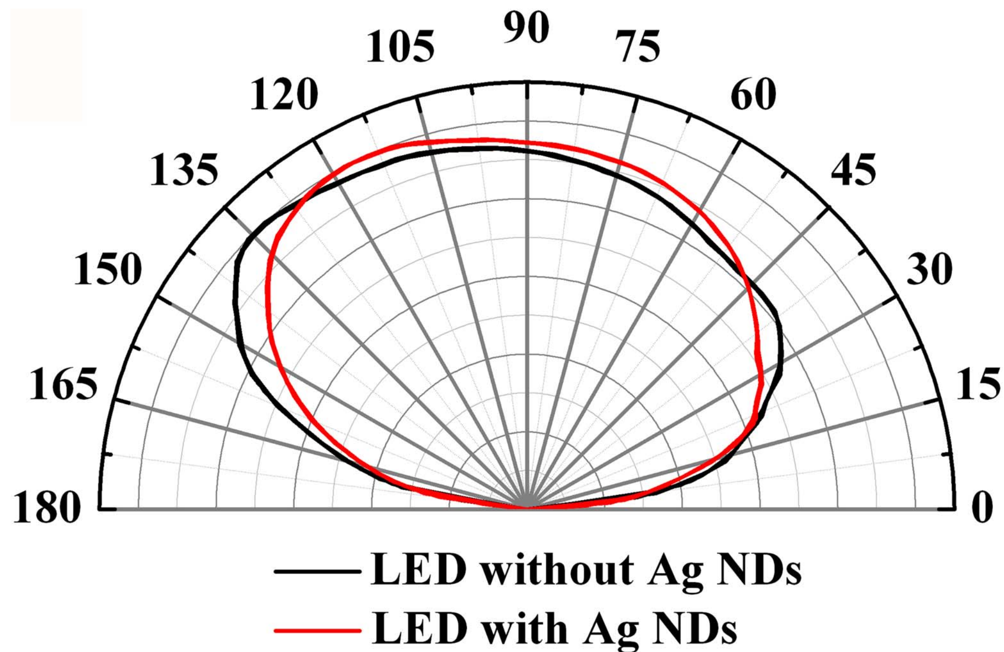

FIG. 6. Far-field emission patterns of the LSP-enhanced LEDs without and with Ag NDs.

the metallic layers[12,21] and the engineering of the surface plasmon dispersion can be achieved by using 2-D lattice resonance. The uncertainty in the Purcell factors in the surface plasmon samples studied here still requires further investigation.

IV. CONCLUSION

In summary, we demonstrated LSP-enhanced InGaN/GaN LED by using Ag NDs embedded in *p*-GaN with a controlled surface coverage. The LSP generated on the Ag NDs was achieved by combining NLL and ICP etching technique, without the use of thermal annealing. The optical output power at a current of 350 mA of the LSP-enhanced LEDs with Ag NDs having a distance of 20 nm and 35 nm to QWs was increased by 26.7% and 31.1%, respectively, compared with that of LED without Ag NDs. Furthermore, the electrical characteristics and optical properties of LSP-enhanced LEDs were found to exhibit a dependence on the distance of between Ag NDs and MQWs region. The Ag NDs arrays also helped to confine the light to radiate in vertical direction for LSP-enhanced LED.

ACKNOWLEDGMENT

This work was supported by the National Natural Sciences Foundation of China under Grant 61274040, 61274008 and 51102226, the National Basic Research Program of China under Grant 2011CB301902, the National High Technology Program of China under Grant 2014AA032605 and Youth Innovation Promotion Association, Chinese Academy of Sciences.

[1] K. Okamoto, I. Niki, A. Shvartser, Y. Narukawa, T. Mukai, and A. Scherer, Nature Mater. **3**, 601 (2004).
[2] G. H. Chan, J. Zhao, E. M. Hicks, G. C. Schatz, and R. V. Duyne, Nano Lett. **7**, 1947 (2007).
[3] C. H. Lu, C. C. Lan, Y. L. Lai, Y. L. Li, and C. P. Liu, Adv. Funct. Mater. **21**, 4719 (2011).
[4] J. H. Sung, J. S. Yang, B. S. Kim, C. H. Choi, M. W. Lee, S. G. Lee, S. G. Park, E. H. Lee, and B. H. O., Appl. Phys. Lett. **96**, 261105 (2010).
[5] D. M. Yeh, C. Y. Chen, Y. C. Lu, C. F. Luang, and C. C. Yang, Nanotechnology **18**, 265402 (2007).
[6] C. Y. Cho, M. K. Kwon, S. J. Lee, S. H. Han, J. W. Kang, S. E. Kang, D. Y. Lee, and S. J. Park, Nanotechnology **21**, 205201 (2010).
[7] M. K. Kwon, J. Y. Kim, B. H. Kim, I. K. Park, C. Y. Cho, C. C. Byeon, and S. J. Park, Adv. Mater. **20**, 1253 (2008).

All article content, except where otherwise noted, is licensed under a Creative Commons Attribution 3.0 Unported license. See: http://creativecommons.org/licenses/by/3.0/
Downloaded to IP: 159.226.231.80 On: Tue, 02 Sep 2014 07:34:08

[8] C. Y. Cho, S. J. Lee, J. H. Song, S. H. Hong, S. M. Lee, Y. H. Cho, and S. J. Park, Appl. Phys. Lett. **98**, 051106 (2011).
[9] Y. Kuo, W. Y. Chang, H. S. Chen, Y. W. Kiang, and C. C. Yang, Appl. Phys. Lett. **102**, 161103 (2013).
[10] L. W. Jang, J. W. Ju, D. W. Jeon, J. W. Park, A. Y. Polyakov, S. Lee, J. H. Baek, S. M. Lee, Y. H. Cho, and I. H. Lee, Opt. Express **20**, 6036 (2012).
[11] J. Henson, J. DiMaria, and R. Paiella, J. Appl. Phys. **106**, 093111 (2009).
[12] J. Henson, J. DiMaria, E. Dimakis, T. D. Moustakas, and R. Paiella, Opt. Lett. **37**, 79 (2012).
[13] C. C. Kao, Y. K. Su, C. L. Lin, and J. J. Chen, IEEE photon. Technol. Lett. **22**, 984 (2010).
[14] T. B. Wei, K. Wu, D. Lan, Q. F. Yan, Y. Chen, C. X. Du, J. X. Wang, Y. P. Zeng, and J. M. Li, Appl. Phys. Lett. **101**, 211111 (2012).
[15] K. Wu, T. B. Wei, D. Lan, X. C. Wei, H. Y. Zheng, Y. Chen, H. X. Lu, K. Huang, J. X. Wang, Y. Luo, and J. M. Li, Appl. Phys. Lett. **103**, 241107 (2013).
[16] T. B. Wei, Q. F. Kong, J. X. Wang, J. Li, Y. P. Zeng, G. H. Wang, J. M. Li, Y. X. Liao, and F. T. Yi, Opt. Express **19**, 1065 (2011).
[17] M. H. Lo, P. M. Tu, C. H. Wang, Y. J. Cheng, C. W. Hung, S. C. Hsu, H. C. Kuo, H. W. Zan, S. C. Wang, C. Y. Chang, and C. M. Liu, Appl. Phys. Lett. **95**, 211103 (2009).
[18] C. Y. Cho, J. J. Kim, S. J. Lee, S. H. Hong, K. J. Lee, S. Y. Yim, and S. J. Park, Appl. Phys. Express **5**, 122103 (2012).
[19] C. K. Choi, Y. H. Kwon, B. D. Little, G. H. Gainer, J. J. Song, S. Keller, U. K. Mishra, and S. P. DenBaars, Phys. Rev. B **64**, 245339 (2001).
[20] T. B. Wei, X. L. Ji, K. Wu, H. Y. Zheng, C. X. Du, Y. Chen, Q. F. Yan, L. X. Zhao, Z. C. Zhou, J. X. Wang, and J. M. Li, Opt. Lett. **39**, 379 (2014).
[21] H. P. Zhao, J. Zhang, G. Y. Liu, and N. Tansu, Appl. Phys. Lett. **98**, 151115 (2011).

All article content, except where otherwise noted, is licensed under a Creative Commons Attribution 3.0 Unported license. See: http://creativecommons.org/licenses/by/3.0/
Downloaded to IP: 159.226.231.80 On: Tue, 02 Sep 2014 07:34:08